A Vehicle Longitudinal Dynamical Model for Propulsion System Tailoring

Toheed Ghandriz, Bengt Jacobson

Division of Vehicle Engineering and Autonomous Systems, Department of Mechanics and Maritime Sciences, Chalmers University of Technology, SE-41296 Gothenburg, Sweden

Abstract

Integrated vehicle–transportation design, based on specific transportation assignments, has resulted in cost- and energy-efficient transport solutions especially in case of battery electric heavy vehicles. This report presents a longitudinal dynamical vehicle model for fast evaluation of the cost function and constraints within a vehicle–transportation optimization. The model includes conventional, fully electric and hybrid vehicles. The presented model evaluates energy consumption and battery degradation on driving cycles with varying speed limit and topography. The energy consumption accuracy of the presented model compared to a high fidelity vehicle model has been seen to be ± 3 % for the tested driving cycles, which can be further improved by tuning parameters.

Keywords: transportation, longitudinal vehicle dynamics, fuel consumption, energy consumption, electric vehicles

1. Introduction

Certain applications related to minimization of a cost function involving road vehicle energy consumption, e.g., routing problem and speed minimization, require quick and relatively accurate evaluation of energy consumption. In addition, optimization of total cost of ownership (TCO) related to integrated vehicle–transportation design requires enormous number of TCO evaluations of different vehicle–configurations of different powertrains. TCO evaluation of heavy vehicles previously was used for example in Davis and Figliozzi (2013), Feng and Figliozzi (2013), Lee et al. (2013), Taefi et al. (2015), Lebeau et al. (2015), Hagman et al. (2016), Taefi et al. (2016), Taefi et al. (2017), and Wadud (2017). In all the mentioned studies vehicles were assumed to operate on flat roads, thus, the road grade was not considered. Moreover, in case of electric vehicles, the mentioned TCO studies simplified the cost of the batteries and battery replacement needed. This report, however, presents a simple model for battery degradation and number of battery replacements. In addition, the vehicle model is sensitive to the type of components used in the powertrain, e.g., size of internal combustion engine (ICE), and size and type of batteries and electric motors, thereby allowing optimum selection of those components by solving an optimization problem, for example according to Ghandriz et al. (2020a) and Ghandriz et al. (2020b). Moreover, a vehicle dynamic model is needed to evaluate driving time, trip time, and performance based characterizations (Edgar et al., 2002; Sadeghi Kati, 2013; Sadeghi Kati et al., 2014; Kharrazi et al., 2015). For electric freight vehicles, trip time is affected by service time, charging power, and the distance to the next charging station.

With the above objectives, a longitudinal vehicle dynamic model was observed to be enough, therefore, lateral dynamics has been neglected assuming that a vehicle is a lumped mass moving on a straight road.

Email addresses: toheed.ghandriz@chalmers.se (Toheed Ghandriz), bengt.jacobson@chalmers.se (Bengt Jacobson)

2. Vehicle dynamic model

Longitudinal equation of motion can be written as follows.

$$F_{wh}(s) = m(s)\,\dot{v}(s) + F_r(s) \tag{1}$$

wherein, $m(s)$, $\dot{v}(s)$ denote mass of the loaded vehicle and acceleration, and $F_{wh}(s)$ denotes the sum of propulsion and brake-actuated longitudinal force over all wheels acting on contact patch of the wheels with the road at traveled distance s, and $F_r(s)$ denotes the resistant force defined by

$$F_r(s) = m(s)\,g\,f_r\,\cos(\phi(s)) + \frac{1}{2}\,\rho_a\,A_f\,c_d\,v(s)^2 - m(s)\,g\,\sin(\phi(s)) \tag{2}$$

wherein, ϕ denotes road grade angle, positive downhill, and g, ρ_a, A_f, c_d, v and f_r denote gravity, air density, front area of the vehicle, aerodynamic drag coefficient, velocity and rolling resistance coefficient, respectively. Rolling resistances are, physically, torques acting on the wheels but their influence here is represented as a force on the vehicle body. Note that velocity should be positive ($0 < v$).

The model is explained treating traveled distance s rather than time t as the independent variable. This is suitable for trajectory optimization over a transport mission as the road angle is described in traveled distance. The conversion from time to space domain is done according to

$$\dot{v}(s) = \frac{dv(s)}{dt} = \frac{dv(s)}{ds}\frac{ds}{dt} = \frac{dv(s)}{ds}v(s) \tag{3}$$

The gross combination mass, i.e., the mass of the loaded vehicle, is described as follows.

$$\begin{aligned} m(s) =& m_v + N_{em}\,m_{ElDrive} + N_{pack}\,m_{pack} + m_{ice} + \\ & m_L(s) - m_U(s) + m_{obl} \end{aligned} \tag{4}$$

wherein, m_v denotes the vehicle curb mass excluding drivelines, powertrain, engines, and battery packs, and N_{em}, $m_{ElDrive}$, N_{pack}, m_{pack}, m_{ice}, $m_L(s)$, $m_U(s)$ and m_{obl} represent number of electric motors, mass of an electric motor and its transmission, number of battery packs, mass of a battery pack, mass of ICE and its associated transmission, mass of loaded freight, mass of unloaded freight and mass of the on-board lift, respectively. If there exists no on-board lift installed on the vehicle then $m_{obl} = 0$. It should be noted that loading-unloading is performed while the vehicle is standing still, i.e., not during the motion, so that $\dot{m}(s) = 0$. Such a definition of the gross combination mass helps evaluation of the vehicle energy consumption in a mission with many nodes where loading–unloading is performed.

Eq. (1) is a differential equation which needs to be integrated; $F_{wh}(s)$ and $\dot{v}(s)$, however, are unknowns. Thus, a speed reference signal $v_{ref}(s)$ needs to be introduced which might not be exactly followed because of the limits of the vehicle powertrain and power sources. Given the reference speed $v_{ref}(s)$ of the driving cycle, the achieved acceleration is calculated as follows.

$$\dot{v}(s) = \begin{cases} \dot{v}_{ref}(s), & F_{wh,min}(s) \le F_{wh}(s) \le F_{wh,max}(s) \\ \dfrac{F_{wh,max}(s) - F_r(s)}{m(s)}, & F_{wh}(s) > F_{wh,max}(s) \\ \dfrac{F_{wh,min}(s) - F_r(s)}{m(s)}, & F_{wh}(s) < F_{wh,min}(s) \end{cases} \tag{5}$$

where, $F_{wh,max}(s)$ and $F_{wh,min}(s)$ are the limits of the longitudinal force delivered by propulsion and braking defined by

$$F_{wh,max}(s) = \min\left(\frac{T_{max}\,Ratio_{max}}{R}, \frac{P_{max}}{v(s)}\right) \tag{6}$$

$$F_{wh,min}(s) = \max\left(\frac{T_{min}\;Ratio_{max}}{R}, \frac{P_{min}}{v(s)}\right) + F_{fri}(s) \tag{7}$$

wherein, T and P are the torque and power produced by electric motors or ICE, acting on wheels, respectively, $Ratio_{max}$ denotes the transmission total final ratio, R denotes the wheel radius, and F_{fri} is the force produced by friction brake.

Furthermore, F_{ice} and F_{em} are defined as propulsion forces actuated by ICE and electric drivelines, respectively, on the contact patch of the wheels as follows.

$$F_{wh}(s) = F_{ice}(s) + n_{em}F_{em}(s) + F_{fri}(s) \tag{8}$$

wherein, n_{em} denotes number of electric motors. The propulsion force is bounded by the powertrain capabilities. Road-wheel grip limit and tire slip models are not considered in this paper, assuming smooth driving on normal road friction.

By calculating the actual speed $v(s)$, using Eq. (5), the travel time on road t_{tor} can be calculated according to

$$t_{tor} = \int_0^{s_f} \frac{ds}{v(s)} \tag{9}$$

wherein, s_f denotes the length of the mission.

2.1. Conventional vehicle and internal combustion engine model

The data for describing different diesel internal combustion engines are provided in terms of highest efficiency versus the normalized power in this paper. A general assumption is that a vehicle is equipped with a tightly stepped gearbox with fast changes, or with a continuous variable transmission (CVT), and the control system keeps the ICE operation on the highest efficiency for each requested power regardless of speed. Figure 1 depicts maximum efficiency versus normalized power $\frac{P_{ice}}{P_{ice,max}}$. The ICE power P_{ice} is described as follows.

$$\begin{aligned} &P_{ice}(s) = \frac{1}{\eta_{ctr}}\, F_{ice}(s)\, v(s) \\ &P_{ice,min} \le P_{ice}(s) \le P_{ice,max} \end{aligned} \tag{10}$$

wherein, η_{ctr} denotes CVT efficiency. For the positive propulsion the ICE power cannot drop below the minimum value shown in Fig. 1. Thus, the following can be used in Eqs. (6) and (7).

$$\begin{aligned} P_{max} &= \eta_{ctr}\, P_{ice,max} \\ P_{min} &= \eta_{ctr}\, P_{ice,min} \\ T_{max} &= \eta_{ctr}\, T_{ice,max} \\ T_{min} &= \eta_{ctr}\, T_{ice,min} \end{aligned} \tag{11}$$

assuming no engine brake is employed.

By change of variable $s = v\,t$, the fuel consumption of one trip F_c is calculated as follows.

$$F_c = \frac{1}{E_{pgf}\,\eta_{ice}\,D_f} \int_0^{t_{tor}} P_{ice}(t)\, dt \tag{12}$$

wherein, η_{ice} denotes the maximum efficiency of ICE, E_{pgf} denotes energy per mass of diesel fuel, D_f represents the fuel density, and t_{tor} is the travel time on road given by Eq. (9). The value of parameters can be found in Ghandriz et al. (2020b).

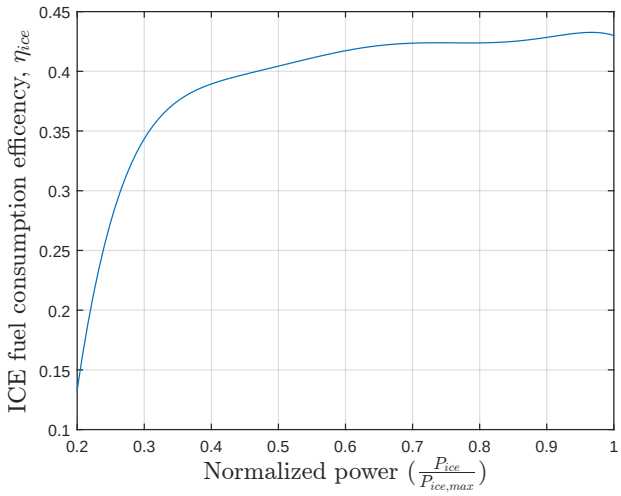

Figure 1: Maximum efficiency against normalized power.

2.2. Fully electric vehicle and electric drive model

Total power P_{em} of an electric motor at position s of the road is given by

$$P_{em}(s) = \begin{cases} \min(\frac{1}{\eta_{tr}} F_{em}(s)\, v(s),\, P_{em,max}), & 0 \leq F_{em}(s) \\ \max(\eta_{tr}\, F_{em}(s)\, v(s),\, P_{em,min}), & F_{em}(s) < 0 \end{cases} \tag{13}$$

wherein, η_{tr} denotes the efficiency of the transmission system of the electric driveline. The charge/discharge power of the battery packs can be calculated as follows.

$$\begin{aligned} P_{bat}(s) &= n_{em}\big(P_{em}(s) + P_{em,loss}(s)\big) + n_{pack} P_{pack,loss}(s) \\ P_{pack,min} &\leq \frac{P_{bat}(s)}{n_{pack}} \leq P_{pack,max} \end{aligned} \tag{14}$$

provided that the state of charge (SoC) of the battery packs is within the limits, i.e.

$$SoC_{min} \leq SoC(s) \leq SoC_{max} \tag{15}$$

wherein, $P_{bat}(s) = n_{pack} P_{pack}(s)$ denotes the total power provided by n_{pack} parallel battery packs, P_{pack} denotes the power of a single battery pack, $P_{em,loss}(s)$ and $P_{pack,loss}(s)$ are positive values accounting for energy losses in the electric motor and a battery pack. Thus, the limits of power and torque acting on the wheels of a fully-electric vehicle can be calculated as

$$\begin{aligned} P_{max} &= \eta_{tr} \min(n_{pack} P_{pack,max} - n_{em} P_{em,loss}(s) - n_{pack} P_{pack,loss}(s), n_{em} P_{em,max}) \\ P_{min} &= \frac{1}{\eta_{tr}} \max(n_{pack} P_{pack,min} - n_{em} P_{em,loss}(s) - n_{pack} P_{pack,loss}(s), n_{em} P_{em,min}) \\ T_{max} &= \eta_{tr}\, n_{em} T_{em,max} \\ T_{min} &= \frac{1}{\eta_{tr}}\, n_{em} T_{em,min} \end{aligned} \tag{16}$$

2.2.1. State of charge and trip time

The electric energy used on a trip, E_{el}, is obtained by relaxing constraint (15) and calculating:

$$E_{el} = \int_0^{t_{tor}} n_{pack} P_{pack}(t)\, dt \tag{17}$$

Moreover, SoC needs to be calculated as follows in order to estimate the feasibility of the selected hardware as well as the charging time spent on a charging station.

$$SoC(s) = SoC(s_i) + \int_{s_i}^{s} \frac{-P_{pack}(S)}{C_{pack}}\, dS, \qquad s_i < s \leq s_{i+1}, \forall i \in \boldsymbol{I}_n \tag{18}$$

wherein, C_{pack} denotes battery packs energy capacity, s_i is the distance of the node i from depot, $\boldsymbol{I}_n$ is the index set of all nodes in the mission, and $SoC(s_i)$ denotes the state of charge of the battery packs right after leaving node i defined as follows.

$$SoC(s_i) = SoC(s_i^-) + \int_0^{t_{ch,i}} \frac{P_{ch,i}(\tau)}{n_{pack} C_{pack}}\, d\tau \tag{19}$$

wherein, $SoC(s_i^-)$ denotes state of charge at arrival to node i, $P_{ch,i}$ is the recharging power from an external source (i.e. charging station at node i) and $t_{ch,i}$ is the charging time. In this paper, recharging power is constant, thus

$$SoC(s_i) = SoC(s_i^-) + \frac{t_{ch,i}\, P_{ch,i}}{n_{pack} C_{pack}} \tag{20}$$

It should be noted that the charging time versus SoC is linear up to approximately 80% of battery capacity, as reported by Montoya et al. (2017). In this paper, batteries are charged up to 90%. The nonlinearity of the additional 10% charging is assumed to have a minor effect.

For a plug-in hybrid vehicle recharging time $t_{ch,i}$ is calculated as follows.

$$t_{ch,i} = \min\big(\max(t_{lu,i}, t_{s,i}), \frac{[SoC_{max} - SoC(s_i^-)]\, n_{pack} C_{pack}}{P_{ch,i}}\big) \tag{21}$$

wherein, t_{lu} denotes loading-unloading time and t_s is a fixed minimum service time. Eq. (21) shows that the charging time ends, if SoC_{max} is reached.

However, an electric vehicle might need to wait longer than the time required for loading-unloading and service time at a node, in order to receive sufficient electric energy that enables it to reach the next charging station. Let define $\Delta SoC(s_{i+1}^-) = SoC(s_{i+1}^-) - SoC(s_i)$ as the charge required to reach node $(i+1)$ from node i. Values of $\Delta SoC(s_{i+1}^-)$ can be calculated in advance by relaxing the constraints $SoC_{min} \leq SoC(s) \leq SoC_{max}$ and simulating the vehicle motion on the road.

In order to be able to reach node $(i+1)$, $\forall i \in \boldsymbol{I}_n$, the following constraint must hold.

$$SoC(s_{i+1}^-) \geq SoC_{min} \tag{22}$$

thus,

$$[\Delta SoC(s_{i+1}^-) + SoC(s_i)] \geq SoC_{min} \tag{23}$$

and using Eq. (20) in Eq. (23), the following inequality is obtained.

$$[\Delta SoC(s_{i+1}^-) + SoC(s_i^-) + \frac{t_{ch,i}\, P_{ch,i}}{n_{pack} C_{pack}}] \geq SoC_{min} \tag{24}$$

thus,

$$t_{ch,i} \geq \frac{[SoC_{min} - \Delta SoC(s_{i+1}^-) - SoC(s_i^-)] n_{pack} C_{pack}}{P_{ch,i}} \tag{25}$$

finally,

$$t_{ch,i} = \begin{cases} \min\Big(\quad \max\big(t_{lu,i}, t_{s,i}, \dfrac{[SoC_{min} - \Delta SoC(s_{i+1}^-) - SoC(s_i^-)]n_{pack}C_{pack}}{P_{ch,i}}\big), \\ \qquad\qquad \dfrac{[SoC_{max} - SoC(s_i^-)]\, n_{pack}C_{pack}}{P_{ch,i}}\Big), \qquad P_{ch,i} > 0 \\ 0, \qquad\qquad\qquad\qquad\qquad\qquad\qquad\qquad \text{otherwise} \end{cases} \tag{26}$$

Based on the described time consuming factors, the trip duration time t_{tr} is defined as follows.

$$t_{tr} = t_{tor} + \sum_{i \in \boldsymbol{I}_n} \max(t_{lu,i}, t_{s,i}, t_{ch,i}) \tag{27}$$

2.2.2. Battery pack energy loss

Following Eq. (14), simple nonlinear energy loss models has been used for electric motors and battery packs similar to the models reported in Ghandriz et al. (2016, 2017). The energy loss in battery packs, with a known resistance R_{bp} is calculated as follows.

$$P_{pack,loss}(s) = I_{pack}(s)^2\, R_{pack}(s) \tag{28}$$

where, I_{pack} is the current given by

$$I_{pack}(s) = \frac{n_{em}(P_{em}(s) + P_{em,loss}(s))}{n_{pack}V_{pack}(s)} \tag{29}$$

wherein, $V_{pack} = 600V$ denotes the voltage of the battery packs. Battery pack resistance and voltage are generally functions of state of charge; but, in this paper, they have been assumed to be constants. Moreover, it is assumed that V_{pack} is considerably larger than the voltage drop because of the battery resistance.

2.2.3. Electric motor energy loss

For calculating $P_{em,loss}$, we assume that the electric motor efficiency is a convex and quadratic function of the electric motor input torque $T(s)$ and speed $\omega(s)$, such that

$$P_{em,loss}(s) = k_\omega\, \omega(s)^2 + k_T\, T(s)^2 \tag{30}$$

Also, we assume that electric motor torque and speed can be regulated in a way that highest efficiency is achieved for a linear relation $T(s) = b\,\omega(s)$, as reported by Ghandriz et al. (2016). Then, lowest power loss of electric motors can be calculated as follows.

$$P_{em,loss}(s) = 2\, k_\omega\, \omega(s)^2 \tag{31}$$

where, ω can be found by

$$\omega(s) = \sqrt{\frac{P_{em}(s)}{b}} \tag{32}$$

wherein, k_ω and $b = \sqrt{\frac{k_\omega}{k_T}}$ denote constants related to characteristics, i.e., efficiency map, of the electric motor. Examples of such values can be found in Ghandriz et al. (2020b).

2.2.4. Battery pack state of health

In addition to the consumed energy, another factor contributing to the ownership cost of an electric vehicle is the battery degradation resulting in battery packs replacement during the service life of the vehicle. In this paper, a state of health model developed for lithium-iron-phosphate battery reported by Wang et al. (2011); Hu et al. (2015) has been implemented. State of health, S_h, of the battery is defined as follows.

$$S_h(t) = 1 - \frac{1}{2\,N_{cycle}\,C_{pack}} \int_0^t (|P_{pack}(\tau)| + |\frac{P_{ch}(\tau)}{n_{pack}}|) d\tau \tag{33}$$

wherein, N_{cycle} denotes number of charge-discharge cycles before end of life of the battery. In general, N_{cycle} is a function of c-rate and various different parameters; in this paper, however, a constant value of 2000 has been considered, despite the fact that N_{cycle} will be larger for future improved batteries.

It should be noted that, battery degradation caused by charging during night, while vehicles are not in operation, should be also considered. Night-charging is needed since batteries must be fully charged at the beginning of operation on the next day. Refer Pelletier et al. (2017) for more models and a review on literatures of battery degradation and behavior.

2.3. Hybrid vehicle dynamic model

In the hybrid vehicle dynamic model the total power must be split between electric motors and ICE. Splitting the power between ICE and electric motors requires an energy management strategy (EMS). A computational-efficient rule-based EMS has been implemented in this paper. (Ghandriz et al., 2017) adapted a predictive EMS validating the results of a rule-based EMS.

Rule-based controller, in short, can be explained as follows. All available electric power must be used. If the available electric power is less than the requested total vehicle power then ICE must be used in parallel, for positive power request. ICE must not work in a power less than a threshold $P_{ice,th}$. $P_{ice,th}$ corresponds to the power where ICE efficiency drops to less than 0.2. In that case, it can be used for charging batteries. For negative power request, batteries could be charged by regenerated energy while braking up to the batteries and electric motors power limits. The excess brake request is handled by friction braking.

2.4. Operating cycle

Operating cycle refers to all information about surrounding environment and road influencing driving situation, (Pettersson, 2017). In this study, the operating cycle has been static and deterministic. Being static means that the input data about a mission and its driving cycle do not evolve in time. The requirement on the operating cycle being static is due to the fact that vehicle design cannot change during operation. Deterministic refers to the input data being known in advance. No level of uncertainty has been considered for the operating cycle. A representative reference speed has been defined to describe the driving situation and traffic. However, no variation in traffic due to nondeterministic events has been taken into account.

In addition to information needed for defining a mission, operating cycle is characterized by topographic data (i.e. elevation, curvature and length of the road) and the reference speed. The reference speed varies in different sections of the road; for example, on rural areas, highway, red light and alongside a curvature, depending on the daily average speed of the respective section. The daily average speed is overridden, while negotiating a curvature, so that the lateral acceleration remains below 1.5 m/s^2. The influence of traffic is not included, which implicitly means that there is no lead vehicle hindering the truck from following the legal speed limit or daily average speed.

3. Simulation result examples

Figure 2 depicts the road elevation, reference and actual velocities generated by simulating a 80 ton conventional vehicle on a road of about 136 km length. The reference speed cannot be followed if the requested power or torque is higher than the powertrain capability, as shown in Fig. 3. Similarly, reference and actual velocities, together with the state of charge, generated by simulating a battery electric vehicle

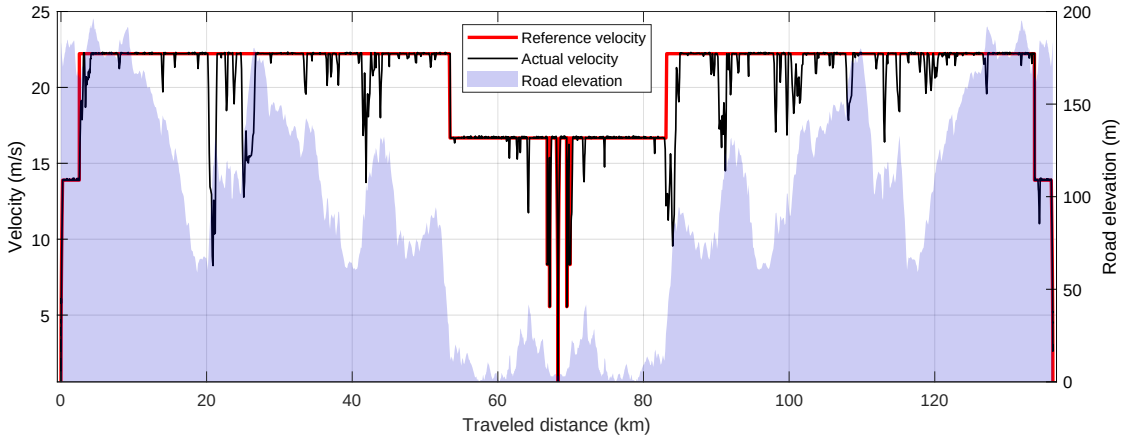

Figure 2: The generated reference and actual velocities as the results of simulating a conventional heavy vehicle.

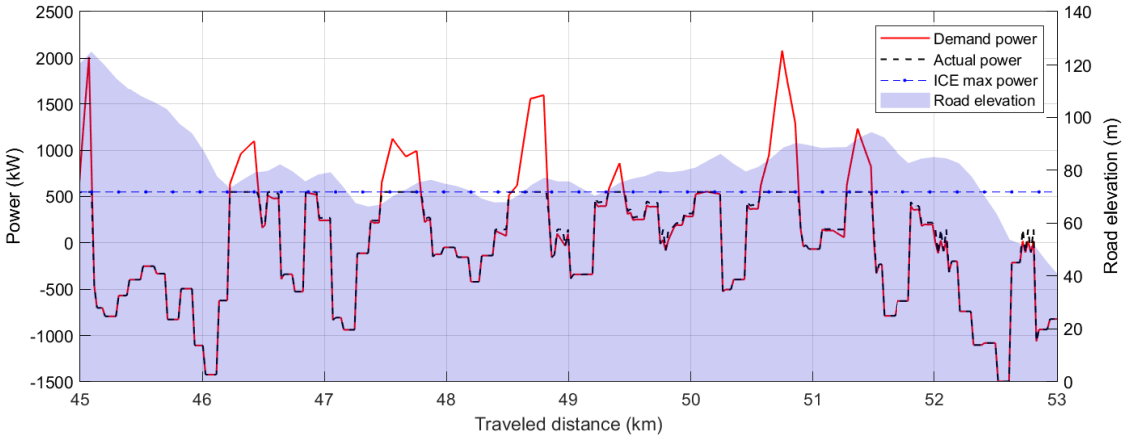

Figure 3: Demand and actual powers, together with ICE maximum power. The actual power is limited by the powertrain capability, i.e., the ICE maximum power considering the transmission power loss. Here, however, the transmission power loss is zero. The power demand is the power needed to reach the requested speed in time step $dt = 1$.

on the same road are shown in Fig. 4. The vehicle is charged in the middle of the road during service time. The power limits of a section of the road is depicted in Fig. 5.

The 80 ton conventional vehicle has a 16 lit engine with maximum power of 550 kW. The electric vehicle has 13 battery packs each having 67.5 kW and 33.75 kW maximum discharge and charge powers, and six electric motors each having 104 kW max power. For both vehicles, the transmission efficiency is assumed to be 1. Refer to Ghandriz et al. (2020b) or Ghandriz et al. (2020a) for physical parameters and detailed vehicle specifications.

Acknowledgment

This work was supported by the Swedish national research program FFI.

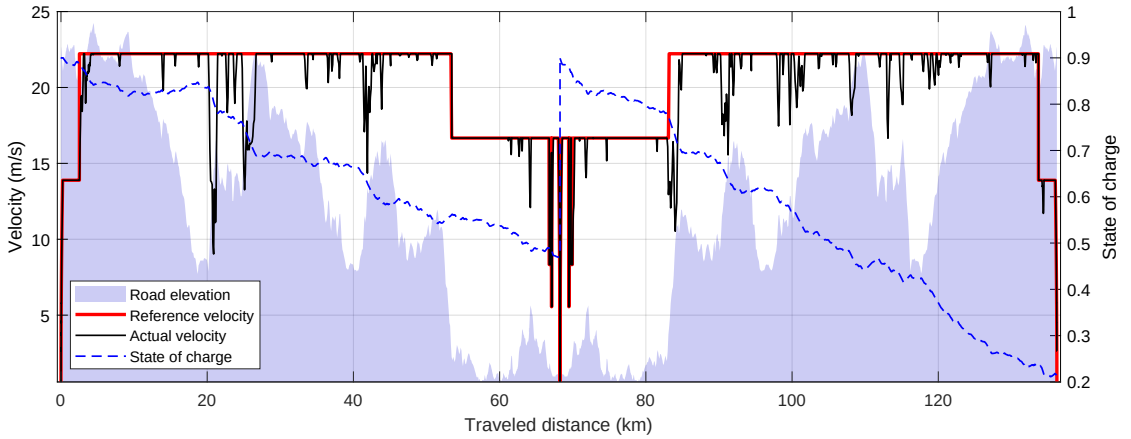

Figure 4: The generated reference velocity, actual velocity and state of charge as the results of simulating a battery electric heavy vehicle. The road and elevation are similar to that in Fig. 2.

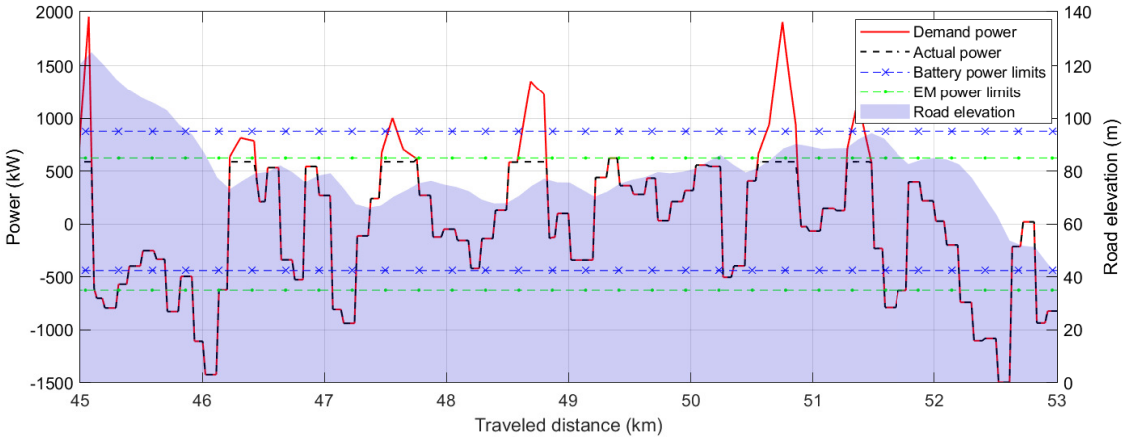

Figure 5: Demand and actual powers, together with power limits of the battery and electric motors (EM). The actual power is limited by the powertrain capability, i.e., the EMs and battery, considering power losses in the transmission, EMs and battery. Here, however, the transmission power loss is zero, but the power losses in EMs and batteries are non-zeros. It should be noted that, for negative power request, friction brake power also helps regenerative brake power if it hits the lower limit.

References

Davis BA, Figliozzi MA (2013) A methodology to evaluate the competitiveness of electric delivery trucks. Transportation Research Part E: Logistics and Transportation Review 49(1):8–23, URL http://dx.doi.org/10.1016/j.tre.2012.07.003

Edgar J, Prem H, Calvert F (2002) Applying performance standards to the Australian heavy vehicle fleet. In: Proceedings of the 7th International Symposium on Heavy Vehicle Weights & Dimensions, Delft, The Netherlands, pp 73–96, URL http://road-transport-technology.org/conferenceproceedings/2000s/ishvwd-7/

Feng W, Figliozzi M (2013) An economic and technological analysis of the key factors affecting the competitiveness of electric commercial vehicles: A case study from the USA market. Transportation Research Part C: Emerging Technologies 26:135–145, URL http://dx.doi.org/10.1016/j.trc.2012.06.007

Ghandriz T, Hellgren J, Islam M, Laine L, Jacobson B (2016) Optimization based design of heterogeneous truck fleet and electric propulsion. In: Intelligent Transportation Systems (ITSC), 2016 IEEE 19th International Conference on, Rio de Janeiro, Brazil, IEEE, pp 328–335, URL http://dx.doi.org/10.1109/ITSC.2016.7795575

Ghandriz T, Laine L, Hellgren J, Jacobson B (2017) Sensitivity analysis of optimal energy management in plug-in hybrid heavy vehicles. In: Intelligent Transportation Engineering (ICITE), 2017 2nd IEEE International Conference on, Singapore, Singapore, IEEE, pp 320–327, URL http://dx.doi.org/10.1109/ICITE.2017.8056932

Ghandriz T, Jacobson B, Hellgren J, Islam M, Laine L (2020a) Transportation-mission-based optimization of heterogeneous heavy-vehicle fleet including electrified propulsion, powertrain tailoring, and fleet sizing. European Transport Research Review (-):Not published

Ghandriz T, Jacobson B, Laine L, Hellgren J (2020b) Impact of automated driving systems on road freight transport and electrified propulsion of heavy vehicles. Transportation Research Part C: Emerging Technologies 115, URL https://doi.org/10.1016/j.trc.2020.102610

Hagman J, Ritzén S, Stier JJ, Susilo Y (2016) Total cost of ownership and its potential implications for battery electric vehicle diffusion. Research in Transportation Business & Management 18:11–17, URL https://doi.org/10.1016/j.rtbm.2016.01.003

Hu X, Johannesson L, Murgovski N, Egardt B (2015) Longevity-conscious dimensioning and power management of the hybrid energy storage system in a fuel cell hybrid electric bus. Applied Energy 137:913–924, URL http://dx.doi.org/10.1016/j.apenergy.2014.05.013

Kharrazi S, Karlsson R, Sandin J, Aurell J (2015) Performance based standards for high capacity transports in Sweden, FIFFI project 2013-03881, report 1: Review of existing regulations and literature URL http://www.diva-portal.org/smash/record.jsf?pid=diva2%3A1168835&dswid=-5021

Lebeau P, Macharis C, Van Mierlo J, Lebeau K (2015) Electrifying light commercial vehicles for city logistics? A total cost of ownership analysis. European Journal of Transport and Infrastructure Research 15(4), URL https://doi.org/10.18757/ejtir.2015.15.4.3097

Lee DY, Thomas VM, Brown MA (2013) Electric urban delivery trucks: Energy use, greenhouse gas emissions, and cost-effectiveness. Environmental science & technology 47(14):8022–8030, URL http://dx.doi.org/10.1021/es400179w

Montoya A, Guéret C, Mendoza JE, Villegas JG (2017) The electric vehicle routing problem with nonlinear charging function. Transportation Research Part B: Methodological 103:87–110, URL http://dx.doi.org/10.1016/j.trb.2017.02.004

Pelletier S, Jabali O, Laporte G, Veneroni M (2017) Battery degradation and behaviour for electric vehicles: Review and numerical analyses of several models. Transportation Research Part B: Methodological 103:158–187, URL http://dx.doi.org/10.1016/j.trb.2017.01.020

Pettersson P (2017) On Numerical Descriptions of Road Transport Missions. Department of Mechanics and Maritime Sciences, Vehicle Engineering and Autonomous Systems, Chalmers University of Technology, URL https://research.chalmers.se/publication/249525

Sadeghi Kati M (2013) Definitions of performance based characteristics for long heavy vehicle combinations. Tech. rep.

Sadeghi Kati M, Fredriksson J, Laine L, Jacobson B (2014) Evaluation of dynamical behaviour of long heavy vehicles using performance based characterstics. In: FISITA 2014 World Automotive Congress-2-6 June 2014, Maastricht, The Netherlands, URL https://research.chalmers.se/en/publication/193707

Taefi TT, Kreutzfeldt J, Held T, Fink A (2015) Strategies to increase the profitability of electric vehicles in urban freight transport. In: E-Mobility in Europe, Springer, Cham, pp 367–388, URL http://dx.doi.org/10.1007/978-3-319-13194-8_20

Taefi TT, Kreutzfeldt J, Held T, Fink A (2016) Supporting the adoption of electric vehicles in urban road freight transport–a multi-criteria analysis of policy measures in Germany. Transportation Research Part A: Policy and Practice 91:61–79, URL http://dx.doi.org/10.1016/j.tra.2016.06.003

Taefi TT, Stütz S, Fink A (2017) Assessing the cost-optimal mileage of medium-duty electric vehicles with a numeric simulation approach. Transportation Research Part D: Transport and Environment 56:271–285, URL http://dx.doi.org/10.1016/j.trd.2017.08.015

Wadud Z (2017) Fully automated vehicles: A cost of ownership analysis to inform early adoption. Transportation Research Part A: Policy and Practice 101:163–176, URL http://dx.doi.org/10.1016/j.tra.2017.05.005

Wang J, Liu P, Hicks-Garner J, Sherman E, Soukiazian S, Verbrugge M, Tataria H, Musser J, Finamore P (2011) Cycle-life model for graphite-lifepo4 cells. Journal of Power Sources 196(8):3942–3948, URL http://dx.doi.org/10.1016/j.jpowsour.2010.11.134